# Epitaxial Electrodeposition of a Crystalline Metal Oxide onto Single-Crystalline Silicon

**Jay A. Switzer,*,† Run Liu,† Eric W. Bohannan,† and Frank Ernst‡**

*Department of Chemistry and Graduate Center for Materials Research, University of Missouri−Rolla, Rolla, Missouri 65409-1170, and Department of Materials Science and Engineering, Case Western Reserve University, 10900 Euclid Avenue, Cleveland, Ohio 44106-7204*

*Received: July 26, 2002; In Final Form: August 30, 2002*

Epitaxial films of cuprous oxide, $Cu_2O$, are electrodeposited from aqueous solution onto single-crystalline Si(001). The epitaxial growth of $Cu_2O$ onto Si is an unexpected result, because there is a strong driving force for the oxidation of Si to form a native amorphous $SiO_2$ layer. The $Cu_2O$ films are single-crystalline in nature, with little or no fiber texture. High-resolution X-ray diffraction shows that the very large lattice mismatch of −21.4% is reduced to +11.2% by the formation of a $Cu_2O(001)[100]//Si(001)[110]$ orientation relationship, in which the film is rotated 45° around the common [001] axis. Cross-sectional transmission electron microscopy studies suggest that the growth mechanism involves an initial electroless deposition of $Cu_2O$ epitaxial seeds in direct contact with the Si(001), with the concomitant oxidation of Si to form a layer of amorphous $SiO_2$ about 3 nm thick. Electrochemical deposition of $Cu_2O$ then proceeds on the epitaxial seeds, with the deposit growing not only perpendicular to the surface but also laterally across the $SiO_2$ interlayer. This type of lateral overgrowth is used in the production of semiconductor-on-insulator (SOI) structures to avoid defects due to misfit strains.

Silicon holds its prominence as a semiconductor in electronic devices in large part because of its propensity to form a native oxide, $SiO_2$, which has superb dielectric properties, and is mechanically and chemically robust.[1] The $SiO_2$ native oxide serves as the capacitor dielectric for information storage in dynamic random-access memories (DRAMs) and as the gate dielectric in complementary metal-oxide semiconductor (CMOS) field-effect transistor (FET) logic devices. As the size of these devices continues to shrink, there is a drive to find alternative dielectric materials with a higher dielectric constant.[1−6] There is also interest in depositing functional metal oxides, such as superconductors, wide-band gap semiconductors, and magnetic materials onto conventional semiconductors. For example, the integration of half-metallic, spintronic materials such as $Fe_3O_4$ with conventional semiconductors such as Si, GaAs, and InP is the focus of much research.[7,8] Here, we show that it is possible to electrodeposit epitaxial films of cuprous oxide, $Cu_2O$, onto single-crystalline Si(001). Because $Cu_2O$ is a wide-band gap semiconductor, it may be possible to produce light-harvesting (e.g., photovoltaic cells) or light-emitting (e.g., LEDs and lasers) devices based on the resulting $Cu_2O$/Si heterojunction. The deposition is performed in a beaker, without the need for expensive ultrahigh-vacuum equipment.

The ease of oxidation of silicon to form the native oxide is a detriment to epitaxial growth on silicon, because the $SiO_2$ layer that forms is amorphous. It is, therefore, quite unexpected that a metal oxide such as $Cu_2O$ can be electrodeposited epitaxially from aqueous solution, because the Si is expected to oxidize and to form an interfacial amorphous $SiO_2$ layer. It is well-known, for example, that trace amounts of metals such as Cu will nucleate onto Si by electroless deposition with the simultaneous oxidation of Si.[9] Kolb and co-workers have shown that epitaxial clusters of Pb, Cu, and Au can be grown on Si by both electroless and electrochemical deposition.[10,11]

We have previously used electrodeposition to form epitaxial films of $\delta$-$Bi_2O_3$,[12] $Cu_2O$,[13,14] ZnO,[15] Pb−Tl−O superlattices,[16] and $Fe_3O_4$[17,18] onto single-crystal Au: a substrate which is relatively inert to oxidation. Lincot et al. have electrodeposited epitaxial films of CdTe on InP(111)[19] and ZnO on GaN(0002),[20] while Moffat has produced epitaxial strained-layer Cu/Ni superlattices on Cu(100).[21] Hence, the electrodeposition of films of metal oxides, compound semiconductors, and metals onto single-crystal surfaces is well-known. The area that is unexplored, however, is the electrodeposition of epitaxial metal oxide films onto Si.

Cuprous oxide is a brick-red, p-type semiconductor with a band gap of 2.1 eV and a dielectric constant of 6.8. There is evidence that Bose-Einstein condensation of excitons can occur in $Cu_2O$ when it is irradiated with high-intensity light.[22,23] We have previously shown that self-assembled layered nanostructures of $Cu_2O$ and Cu can be used to produce a resonant tunneling device that exhibits negative differential resistance at room temperature.[24,25] Cuprous oxide has a primitive cubic structure with space group *Pn*3*m*, and a lattice parameter of 0.427 nm. In addition to the issue of depositing the epitaxial metal oxide onto a highly reducing substrate like Si, the $Cu_2O$/Si epitaxial system is also interesting because of its large lattice mismatch of −21.4%. It is often (incorrectly) believed that epitaxy can only be achieved in systems with small lattice mismatch.

Epitaxial films of $Cu_2O$ were deposited onto p-type Si(001) from an aqueous solution of 0.4 M Cu(II) and 3 M lactate ions at pH 9 using a bath temperature of 65 °C. The Si(001) wafers were supplied by Virginia Semiconductor doped with boron to a resistivity of 7.5 Ω cm, corresponding to a hole density of about $2 \times 10^{15}$ $cm^{-3}$. Although results in this Letter are

* Author to whom correspondence should be addressed. E-mail: jswitzer@umr.edu.
† University of Missouri−Rolla.
‡ Case Western Reserve University.

10.1021/jp0266188 CCC: $22.00 
Published on Web 11/12/2002

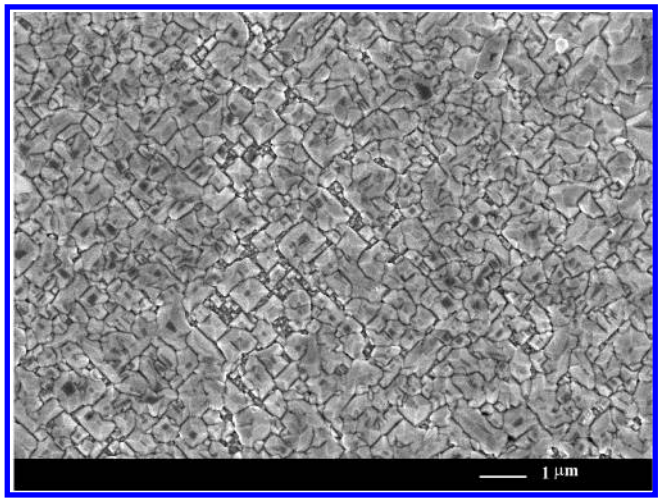


**Figure 1.** Scanning electron micrograph (SEM) image of a 2 $\mu$m-thick film of $Cu_2O$ on Si(001).

presented only for p-type Si, we have also observed epitaxial growth on n-type Si(001). The wafers were degreased in ethanol and acetone and then rinsed with HPLC water before etching to produce a H-terminated surface. The etch consisted of 5% HF for 1 min, hot HPLC water for 15 min, and 5% HF for 10 s, followed by a thorough washing with HPLC water. The H-terminated surface produced by this treatment is stable enough that the wafers can be handled in air.[26,27] Ohmic contacts were made using Ga−In eutectic. The wafers were placed in the deposition bath at open circuit for approximately 10 s before applying the electrode potential of −0.45 V vs the standard calomel electrode (SCE). This potential corresponds to an overpotential for $Cu_2O$ deposition of approximately −385 mV.[14] A plan-view scanning electron micrograph (SEM) image of a film that is approximately 2 $\mu$m thick is shown in Figure 1. The in-plane order of the film is evident in the SEM image. The surface is covered with aligned pyramids ranging in size from 0.5 to 1 $\mu$m.

The epitaxial nature of the $Cu_2O$ film was verified by X-ray diffraction (XRD) using a high-resolution four-circle diffractometer (Philips X′Pert MRD). The Bragg−Brentano scans in Figure 2a probe the out-of-plane orientation of the film. Only the (002) and (004) peaks for $Cu_2O$ are observed. A rocking scan of the $Cu_2O$(002) peak has a full width at half-maximum (fwhm) of 2.01°, compared with a fwhm of 0.007° for the Si-(004) peak. The rocking scan indicates that the $Cu_2O$ has a slight mosaic spread. The lattice parameter for the $Cu_2O$ of 0.4269 nm agrees well with the known bulk lattice parameter, indicating that the majority of the film is completely relaxed. The in-plane orientation of the film was probed by pole figures and azimuthal scans. In a pole figure, planes other than those parallel with the substrate surface are probed by selecting the Bragg angle, $\theta$, for the plane of interest and then tilting the sample through a series of tilt angles, $\chi$, and rotating the sample through azimuthal angles, $\phi$, from 0 to 360°. Peaks occur in the pole figure when the Bragg condition is satisfied. Figure 2b shows a (220) pole figure for $Cu_2O$ that was obtained by setting $2\theta = 61.344°$ for the (220) planes of $Cu_2O$. Four sharp spots are seen in the pole figure at $\chi = 45°$, corresponding to the angle between {100} and {220} planes in a cubic system. A [001] fiber texture (that is, a film that is oriented [001] out-of-plane, but is randomly oriented in-plane) would produce a ring pattern in the pole figure. The in-plane orientation of the film relative to the Si-(001) substrate is determined from the azimuthal scan in Figure 2c. An azimuthal scan is a two-dimensional cross section at a

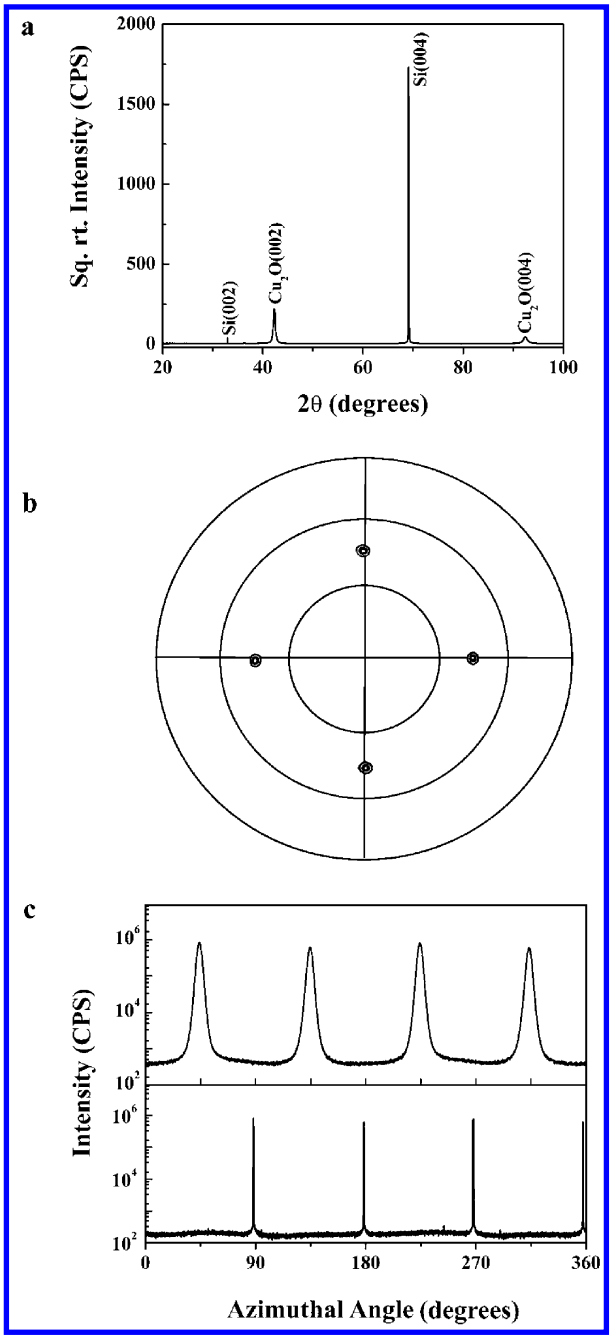


**Figure 2.** X-ray diffraction scans of the epitaxial $Cu_2O$ film on Si-(001). Bragg−Brentano $\theta/2\theta$ scan (a) probing the out-of-plane orientation of the film. Only the (002) and (004) peaks for $Cu_2O$ are observed. A rocking scan of the $Cu_2O$(002) peak has a full width at half-maximum of 2.01°, indicating a slight mosaic spread. A (220) pole figure (b) of the $Cu_2O$ film showing only a [001] orientation. The radial grid lines on the pole figure correspond to 30° increments of the tilt angle. The four spots are at $\chi = 45°$, corresponding to the angle between (100) and (220) planes. The sharp spots are due to the single-crystal nature of the film, because a film with a [001] fiber texture would show a ring at this tilt angle. Azimuthal scans (c) probing the in-plane orientation of the $Cu_2O$ film (top) relative to the Si substrate (bottom). The (111) planes of Si at $2\theta = 28.433°$ and $Cu_2O$ at $2\theta = 36.418°$ were brought into the Bragg condition by tilting the sample at $\chi = 54.7°$ and rotating the sample through azimuthal angles, $\phi$, of 0 to 360°. Notice that the $Cu_2O$ peaks are rotated 45° relative to those of Si, consistent with a $Cu_2O$(001)[100]//Si(001)[110] orientation relationship. The X-ray radiation was Cu $K_{\alpha 1}$ with $\lambda = 0.154056$ nm.

fixed $\chi$ of a three-dimensional pole figure. The azimuthal scans in Figure 2c were obtained by selecting the Si(111) planes at $2\theta = 28.433°$ and the $Cu_2O$(111) planes at $2\theta = 36.418°$ and

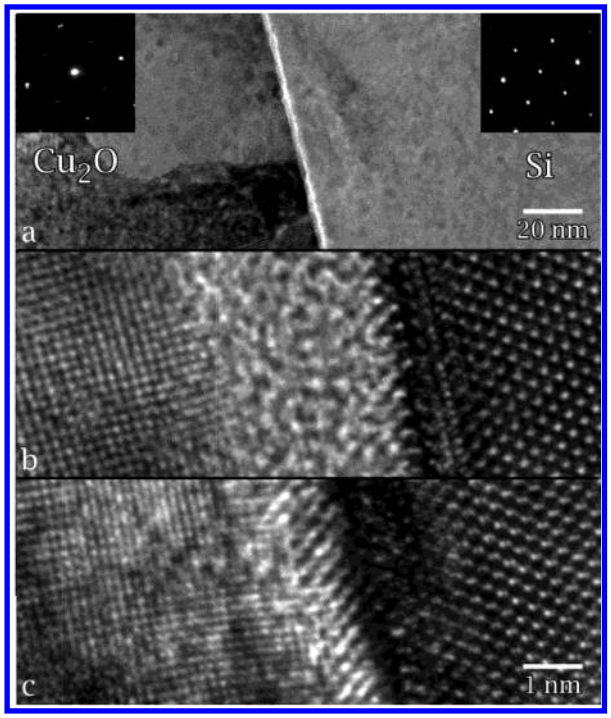


**Figure 3.** Cross-sectional transmission electron micrograph (TEM) images of the $Cu_2O$/Si interface. Conventional TEM bright-field image (a), showing that the two materials are separated by an interlayer of a different less-scattering material. The diffraction patterns shown in the insets indicate that the viewing direction corresponds to [100] in the $Cu_2O$ and [110] in the Si, and that the [001] normal of the Si substrate corresponds to a [001] direction in the $Cu_2O$. High-resolution TEM image (b) of the $Cu_2O$/Si interface. The image confirms the orientation relationship indicated by the X-ray and electron diffraction patterns. The image also shows that the interlayer is about 3 nm thick and is amorphous. High-resolution TEM image (c) in another region of the sample in which the $Cu_2O$ is in direct contact with the Si.

tilting the sample at $\chi = 54.7°$ (the angle between {111} and {100} planes in a cubic system). The azimuthal scans show that the $Cu_2O$ film is rotated by 45° about the [001] axis relative to the Si substrate. Also, it should be noted that the baseline in the $Cu_2O$ azimuthal scan is only about 0.06% of the height of the $Cu_2O$ peaks, again indicating that the sample is single-crystal-like, with very little fiber texture. An epitaxial relationship consistent with the azimuthal scan is $Cu_2O(001)[100]//Si(001)[110]$. The 45° rotation of the film relative to the substrate lowers the lattice mismatch of the corresponding interatomic spacings parallel to the interface from −21.4% (in the case of parallel lattices) to 11.2%.

The $Cu_2O$/Si interface was studied by cross-sectional transmission electron microscopy (TEM). Figure 3a shows a conventional TEM bright-field image, revealing that the two materials are separated by an interlayer of a different less-scattering material. The diffraction patterns in the insets of Figure 3a indicate that the viewing direction corresponds to [100] in $Cu_2O$ and [110] in Si, and that the [001] normal of the Si corresponds to the [001] direction in $Cu_2O$. These diffraction patterns are consistent with the $Cu_2O(001)[100]//Si(001)[110]$ orientation relationship determined by XRD. Figure 3b shows a high-resolution TEM (HRTEM) image of the interface, obtained with a Tecnai F30 (FEI) field-emission TEM. The image confirms the relationship indicated by the X-ray and electron diffraction patterns. It also shows that the interlayer is 3 nm thick. The brighter appearance and the speckle pattern of the interlayer in the HRTEM image both suggest that the interlayer is amorphous. High-resolution electron spectroscopic imaging (ESI) and X-ray energy dispersive spectroscopy (XEDS) results are consistent with this interlayer being an amorphous layer of $SiO_2$. Although one interpretation of these results would be that the $Cu_2O$ is deposited onto a 3 nm thick native oxide of $SiO_2$ on Si, it is unlikely that the orientation information could be transmitted through the amorphous layer. Careful study of the sample shows that there are small regions in which the $Cu_2O$ is in direct contact with the Si. One of these contact points, or seeds, is shown in the HRTEM image in Figure 3c. The diameter of these contact points is estimated from HRTEM to be about 10 nm.

The mechanism we propose for the formation of epitaxial $Cu_2O$ films on Si is shown in Figure 4. The initial deposition is electroless, in which the Cu(II) ions are reduced by the Si to produce epitaxial $Cu_2O$ seeds, with the concomitant oxidation of Si to $SiO_2$ between the seeds. There is a very large thermodynamic driving force for this electroless deposition, and it is similar to what has been observed earlier for the electroless deposition of metals onto Si.[9−11] Consistent with electroless deposition, a Si wafer immersed in the deposition solution attains

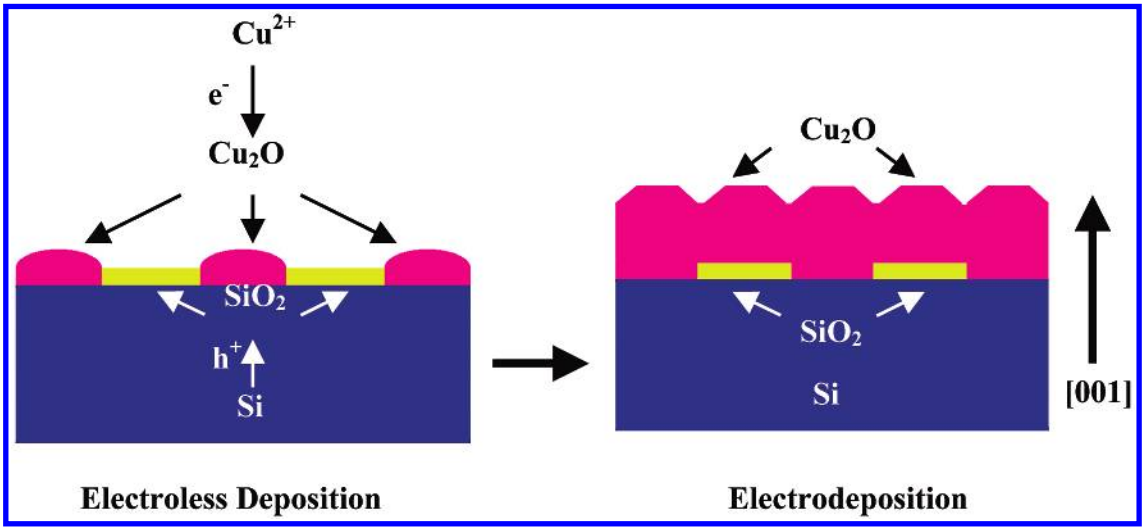


**Figure 4.** Proposed scheme for the production of epitaxial $Cu_2O$ on Si(001). There is an initial electroless deposition in which the Cu(II) is reduced to epitaxial $Cu_2O$ seeds by the Si, with the concomitant oxidation of Si to $SiO_2$. The $Cu_2O$ seeds are surrounded by a layer of $SiO_2$ about 3 nm thick. The electrodeposition then proceeds on the $Cu_2O$ epitaxial seeds. During the electrodeposition, the $Cu_2O$ grows in the [001] direction, in addition to lateral overgrowth on the $SiO_2$ layer. Defects due to strain relief should be localized at the $Cu_2O$/Si contact points.

the open-circuit potential of bulk $Cu_2O$ within a few seconds. Electrochemical deposition of $Cu_2O$ then proceeds on the $Cu_2O$ seeds, with the deposit growing not only perpendicular to the surface but also laterally over the $SiO_2$ interlayer. This type of lateral overgrowth has been used before by Bauser and co-workers in the epitaxial growth of semiconductor-on-insulator (SOI) structures by liquid-phase epitaxy.[28,29] An advantage of SOI structures is that the outer semiconductor layer is nearly defect free, because defects such as misfit dislocations due to strain relief are localized at the small contact points. The majority of the epitaxial film grows dislocation-free on the amorphous $SiO_2$ interlayer. As in van der Waals epitaxy,[30,31] this type of epitaxial growth should permit accommodation of large lattice mismatch due to the lack of a templating effect of the amorphous $SiO_2$ layer.

The results we have presented here demonstrate that it is possible to electrodeposit epitaxial metal oxide films onto single-crystalline Si. We expect that the method is applicable to the production of other morphologies and other metal oxides. For example, although this study emphasized the deposition of highly ordered continuous films, it should be possible to electrodeposit epitaxial nanowires from the electrolessly deposited seeds by minimizing lateral overgrowth. Our proposed mechanism suggests that oxides such as ZnO[15,20] which are electrodeposited cathodically should be easier than anodically formed materials to grow as epitaxial films on Si, but we are also studying the electrodeposition of $CeO_2$ and $Fe_3O_4$ onto Si. $CeO_2$ is a high dielectric material which is lattice matched to Si. $Fe_3O_4$ is a spintronic metal oxide that we wish to integrate with conventional semiconductor devices.[7,8,17,18] There is interest in depositing this material not only onto Si, but also onto GaAs and InP. Preliminary results from our laboratory have shown, for example, that epitaxial films of both $Cu_2O$ and $Fe_3O_4$ can be electrodeposited onto single-crystal InP(001).

**Acknowledgment.** This work was supported by National Science Foundation Grants CHE-9816484, DMR-0071365, and DMR-0076338. We thank N. Zheng of Case Western Reserve University for the TEM sample preparation.

## References and Notes

(1) Kingon, A. I.; Maria, J.-P.; Streiffer, S. K. *Nature* **2000**, *406*, 1032.
(2) McKee, R. A.; Walker, F. J.; Chisholm, M. F. *Science* **2001**, *293*, 468.
(3) Yu, Z.; Ramdani, J.; Curless, J. A.; Overgaard, C. D.; Finder, J. M.; Droopad, R.; Eisenbeiser, K. W.; Hallmark, J. A.; Ooms, W. J.; Kaushik, V. S. *J. Vac. Sci. Technol. B* **2000**, *18*, 2139.
(4) Niu, F.; Hoerman, B. H.; Wessels, B. W. *J. Vac. Sci. Technol. B* **2000**, *18*, 2146.
(5) Hong, M.; Kwo, J.; Kortan, A. R.; Mannaerts, J. P.; Sergent, A. M. *Science* **1999**, *283*, 1897.
(6) Norton, D. P.; Pearton, S. J.; Christen, H. M.; Budai, J. D. *Appl. Phys. Lett.* **2002**, *80*, 106.
(7) Prinz, G. A. *Science* **1998**, *282*, 1660.
(8) Wolf, S. A.; Awschalom, D. D.; Buhrman, R. A.; Daughton, J. M.; Molnár, S. von; Roukes, M. L.; Chtchelkanova, A. Y.; Treger, D. M. *Science* **2001**, *294*, 1488.
(9) Homma, T.; Wade, C. P.; Chidsey, C. E. D. *J. Phys. Chem. B* **1998**, *102*, 7919.
(10) Ziegler, J. C.; Reitzle, A.; Bunk, O.; Zegenhagen, J.; Kolb, D. M. *Electrochim. Acta* **2000**, *45*, 4599.
(11) Ziegler, J. C.; Scherb, G.; Bunk, O.; Kazimirov, A.; Cao, L. X.; Kolb, D. M.; Johnson, R. L.; Zegenhagen, J. *Surf. Sci.* **2000**, *452*, 150.
(12) Switzer, J. A.; Shumsky, M. G.; Bohannan, E. W. *Science* **1999**, *284*, 293.
(13) Bohannan, E. W.; Shumsky, M. G.; Switzer, J. A. *Chem. Mater.* **1999**, *11*, 2289.
(14) Switzer, J. A.; Kothari, H. M.; Bohannan, E. W. *J. Phys. Chem. B* **2002**, *106*, 4027.
(15) Liu, R.; Vertegel, A. A.; Bohannan, E. W.; Sorenson, T. A.; Switzer, J. A. *Chem. Mater.* **2001**, *13*, 508.
(16) Kothari, H. M.; Vertegel, A. A.; Bohannan, E. W.; Switzer, J. A. *Chem. Mater.* **2002**, *14*, 2750.
(17) Nikiforov, M. P.; Vertegel, A. A.; Shumsky, M. G.; Switzer, J. A. *Adv. Mater.* **2000**, *12*, 1351.
(18) Sorenson, T. A.; Morton, S. A.; Waddill, G. D.; Switzer, J. A. *J. Am. Chem. Soc.* **2002**, *124*, 7604.
(19) Lincot, D.; Kampmann, A.; Mokili, B.; Vedel, J.; Cortes, R.; Froment, M. *Appl. Phys. Lett.* **1995**, *67*, 2355.
(20) Pauporte, Th.; Lincot, D. *Appl. Phys. Lett.* **1999**, *75*, 3817.
(21) Moffat, T. P. *J. Electrochem. Soc.* **1995**, *142*, 3767.
(22) Snoke, D. *Science* **1996**, *273*, 1351.
(23) Johnsen, K.; Kavoulakis, G. M. *Phys. Rev. Lett.* **2001**, *86*, 858.
(24) Switzer, J. A.; Hung, C.-J.; Huang, L.-Y.; Switzer, E. R.; Kammler, D. R.; Golden, T. D.; Bohannan, E. W. *J. Am. Chem. Soc.* **1998**, *120*, 3530.
(25) Switzer, J. A.; Maune, B. M.; Raub, E. R.; Bohannan, E. W. *J. Phys. Chem. B* **1999**, *103*, 395.
(26) Allongue, P.; Kieling, V.; Gerischer, H. *Electrochim. Acta* **1995**, *40*, 1353.
(27) Higashi, G. S.; Chabal, Y. J.; Trucks, G. W.; Raghavachari, K. *Appl. Phys. Lett.* **1990**, *56*, 656.
(28) Bergmann, R.; Bauser, E.; Werner, J. H. *Appl. Phys. Lett.* **1990**, *57*, 351.
(29) Hansson, P. O.; Bergmann, R.; Bauser, E. *J. Crystal Growth* **1991**, *114*, 573.
(30) Koma, A.; Yoshimura, K. *Surf. Sci.* **1986**, *174*, 556.
(31) Löher, T.; Tomm, Y.; Pettenkofer, C.; Giersig, M.; Jaegermann, W. *J. Crystal Growth* **1995**, *146*, 408.